

Liquid Plasma Sprayed Coatings of Yttria-Stabilized Zirconia for SOFC Electrolytes

R. Rampon, F.-L. Toma, G. Bertrand, and C. Coddet

(Submitted February 27, 2006; in revised form April 28, 2006)

To achieve solid oxide fuel cells (SOFC) at reduced costs, the atmospheric plasma spray (APS) process could be an attractive technique. However, to make dense and thin layers as needed for electrolytes, a suspension is preferably implemented as a feedstock material instead of a conventional powder. Suspensions of yttria-stabilized zirconia particles in methanol have been prepared with various solid loadings and states of dispersion. An external injection system was used to ensure the atomization and radial injection of the suspension into the Ar-H₂ plasma under atmospheric conditions. The coatings morphologies were characterized by scanning electron microscopy, and their porosity was evaluated by the Archimedes method. Differences in the microstructure of the deposits were observed depending on the APS operating conditions. Special attention has been dedicated to assess the influence of the suspension as well as the injection on the layer morphology. For this purpose, the atomization has been investigated and efforts have been made to understand relationships among suspension properties, atomization, and coating microstructure.

Keywords liquid plasma spray, solid oxide fuel cell, yttria-stabilized zirconia

1. Introduction

More and more attention is paid to alternative means of energy production among which fuel cells seem to be a very attractive and a very effective energy-conversion device. Indeed, fuel cells have many advantages compared with conventional electrical power generation systems, such as high conversion efficiency and environmental compatibility. Solid oxide fuel cells (SOFC) have potential benefits because of their compatibility with various fuels, their ability to coproduce electricity and heat, their high electric efficiency, and their low NO_x and SO_x emissions. The SOFC performance strongly depends on the morphology and composition of the electrodes as well as the electrolyte. Cubic zirconia 100 to 150 μm thick stabilized with 8 mol.% yttria is commonly used as electrolyte material in SOFC due to its attractive ionic conductivity at a high operating temperature (1000 °C) (Ref 1). Such high thermal load of the materials used in SOFC components can result in detrimental diffusion and evaporation processes with a strong reduction of the cell performance and reduced long-term stability. To increase stability and lifetime, the operating temperature of the cells has to be reduced to about 700 °C. To achieve this, it is necessary to decrease the thickness of the zirconia-based electrolyte. The new thin (around 10 to 20 μm) electrolyte layer should be fully dense to

obtain improved gas tightness and reduced internal resistant loss.

Numerous conventional fabrication processes (tape casting, screen printing) have been investigated to produce the proposed electrolyte, but these techniques require long processing times (>10 h) and expensive post thermal treatment (sintering of YSZ is above 1400 °C) to ensure good performance. In the last few years, many attempts have been made to produce SOFC layers using thermal spray technologies. Fauchais et al. (Ref 2, 3), Gitzhofer et al. (Ref 4, 5), Moreau et al. (Ref 6, 7), Stover et al. (Ref 8, 9), Schiller et al. (Ref 10, 11), and Ma et al. (Ref 12, 13) have used APS by conventional or new plasma torches, vapor plasma spraying (VPS), or suspension plasma spraying (SPS) via direct current (DC) or RF plasma guns to produce electrodes, electrolyte, or complete cells. Plasma spraying has thus emerged as a quick and relatively inexpensive process for the fabrication of YSZ electrolyte. However, due to the numerous defects (interlamellar pores and microcracks) introduced in the plasma sprayed layer, these techniques still need significant improvements to provide dense and thin coatings without the need for a post heat treatment. Among all these technologies, the SPS, recently developed to spray finely structured coatings by injecting, instead of microsized powders, a suspension of nanosized particles in a DC plasma jet seems to be the most promising method (Ref 14-17). This process requires a suspension of nanometric particles in a solvent (aqueous or organic). A dispersant is often necessary to achieve a high state of dispersion and stability by enhancing the repulsive interactions between particles. The control of the suspension characteristics and behavior is the most important point for SPS because these properties highly influence the atomization of the suspension and the drop penetration in the plasma jet and consequently the microstructural features of the coating.

The current study focuses on the relationship among the different properties of the suspensions used as feedstock material, the injection parameters into the plasma jet, and the microstructural characteristics of the resulting coatings.

This article was originally published in *Building on 100 Years of Success, Proceedings of the 2006 International Thermal Spray Conference* (Seattle, WA), May 15-18, 2006, B.R. Marple, M.M. Hyland, Y.-Ch. Lau, R.S. Lima, and J. Voyer, Ed., ASM International, Materials Park, OH, 2006.

R. Rampon, F.-L. Toma, G. Bertrand, and C. Coddet, LERMPS-UTBM, Site de Sévenans, 90010 Belfort, France. Contact e-mail: ghislaine.bertrand@utbm.fr.



2. Experimental Procedure

The spraying system comprises a conventional atmospheric plasma torch PTF4 B (Sulzer Metco, Winterthur, Switzerland) installed on an ABB robot to control the trajectory. Plasma gases flow rates and arc current were, respectively, 30 sLpm for Ar, 8 sLpm for H₂, and 600 A. Two standoff distances were adopted in the current study: 40 mm, which is commonly used in the SPS process, and 60 mm, which gave good results as can be seen in already published work on dense TiO₂ layers made with the same feedstock injection device (Ref 18). A homemade external injection system was used to ensure the atomization and radial injection of the suspension into the Ar-H₂ plasma under atmospheric conditions. For atomization, a two-fluid nozzle was designed and used. In this atomization device, the energy for atomization is provided by the rapid expansion of a gas (Ar) that is mixed with the suspension within the body of the nozzle (internal mixing) (Ref 18). The mechanically stirred suspension was introduced using a peristaltic pump in the injector-atomizer nozzle, which is positioned onto a standard ring fixed on the plasma torch. Suspension feed rates and Ar atomizing gas flow rates were adjusted to change the atomized droplets size.

Stainless steel substrates (316L) are fixed on a circular substrate holder that is rotating while the torch moves parallel to the support axis. Cooling devices (Venturi systems) were also used. The substrates were sand blasted beforehand with corundum particles of 250 μm.

Suspensions of yttria-stabilized zirconia powders, from Saint-Gobain (Le Pontet, France) (d_{50} 0.6 μm), in methanol have been prepared with various solid loadings. Several dispersants were evaluated, but in the present work only Solsperse 20000, from Noveon (Manchester, UK), was used. The suspension characteristics and behavior were evaluated performing sedimentation tests using the TurbiScan Laboratory Expert apparatus (Formulation, Lunion, France). To study the sedimentation rates and the settling volumes for long times, the suspension that was poured into a tube was crossed by a near-infrared (IR) light (880 nm), and the intensities of the backscattered and transmitted lights were measured versus time. Viscosity measurements were also carried out on VISCO88BV device from Malvern Instruments (Worcestershire, UK) at 1230 s⁻¹ shear rate (21.2 °C).

The drop sizes, before entering the plasma, have been investigated using the Spraytech (Malvern France) system, the measurement principle of which is based on laser light scattering (Mie diffraction theory). These experiments were limited in the upper size at 400 μm due to the chosen lens. Various parameters were evaluated, such as the argon atomizing gas flow rate, the suspension feed rate, the suspension formulation, and the injector design. The ratio between the suspension feed rate and the argon flow rate, noted RSG, was varied from 100 to 200 and 400 by adjusting the suspension output at 40 and 20 mL/min and the gas rate at 4 and 8 sLpm. For each suspension, the droplet size distribution was determined as a function of this parameter.

The coatings morphologies were characterized by scanning electron microscopy (SEM), using a JEOL JSM 5800LV (JEOL, Tokyo, Japan) microscope. Archimedes porosity was also carried out on free-standing coatings (the substrates were dissolved in a mixture of nitric and hydrochloric acids), but due to the

Table 1 Suspensions formulation, atomization parameter and spraying conditions

Suspension (solid loading), wt.%	RSG	Spraying distance, mm
20	100	60
20	100	40
20	400	40
20	400 (flow rate doubled)	40
60 + 4 dispersant	400	40
20(a) (powder d_{50} 0.47 μm)	100	40

Note: Ar, 30 sLpm; H₂, 8 sLpm; 1:600 A. (a) Powder d_{50} , 0.47 μm

thinness of the coatings these often cracked, thus creating new artificial porosity.

Spraying conditions, suspension compositions, and injection parameters evaluated in the current study are presented in Table 1.

3. Results and Discussion

3.1 Suspension Characteristics

Various solid loadings from 10 to 60 wt.% were evaluated using the sedimentation test previously described to assess the stability of the suspensions. In Fig. 1 the relative sedimentation height (which is the ratio between the sediment height and the initial suspension height, or RSH) is reported versus time. The destabilization starts after 10 min for the suspensions with 10, 20, and 40 wt.% YSZ, and it ends after, respectively, 10, 20, and 25 min. The suspension with 60 wt.% loading has a constant sedimentation rate around 0.08% min⁻¹ for 180 min. The stability duration is increasing with the loading. At the same time, the viscosity of the suspensions increases with the solid loading: 3 cP for 10 wt.%, 4 cP for 20 wt.%, 6 cP for 40 wt.%, and 12 cP for 60 wt.%.

It was also noticed that the 20 wt.% YSZ suspension shows a bimodal size distribution before the sedimentation occurs (first peak at 1 μm and second peak at 3 μm) that is evolving during sedimentation toward large particle sizes (first peak at 1.5 μm and second peak at 10 μm) (Fig. 2). This denotes the flocculation of the fine particles as well as a poor stability.

A dispersant, Solsperse 20000, was added and an increase of the stability was noted with the amount of dispersant (Fig. 3). The maximum stability for a 60 wt.% YSZ suspension was achieved with the addition of 4 wt.% dispersant. This enhanced stability could be related to an improvement of the dispersion state of the suspension. This behavior seems to be corroborated by the viscosity measurements: 12 cP without dispersant, 11 cP with 2 wt.% Solsperse 20000, and 9 cP with 4 wt.%.

3.2 Evolution of the Droplet Size Distribution

The influence of the argon (atomizing gas) flow rate and the suspension feed rate on the droplet size distribution was studied using the critical operating parameter, RSG, previously precised. The effect of its variation during the atomization of a 20 wt.% suspension is shown in Fig. 4. The major consequence of the RSG increase is to move the droplet size distribution toward a small size. Also, the size distribution seems to be narrow. Indeed, at RSG of 100, the distribution size can be regarded as bimodal (some droplets were too large to be detected) with the major peak at 250 μm and the peak shoulder around 60 μm.

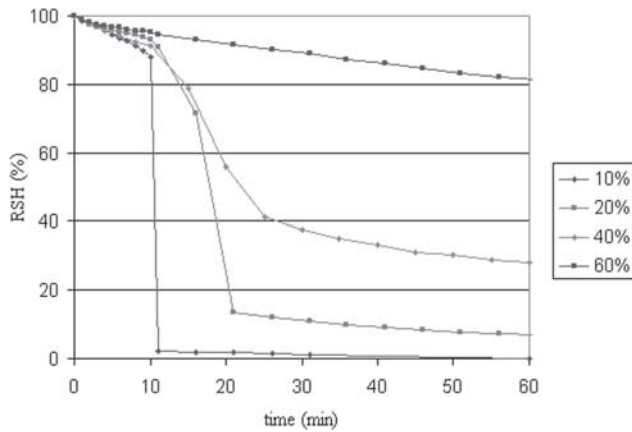


Fig. 1 Evolution of the sediment heights versus time for various solid loading

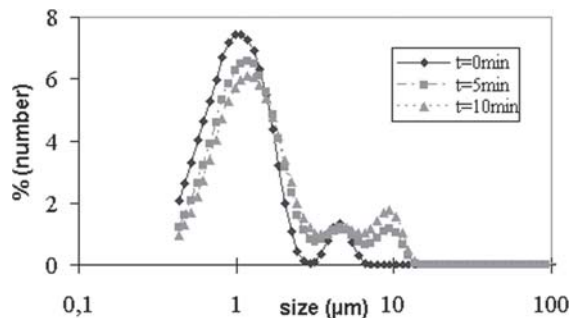


Fig. 2 Evolution of the particle sizes distribution in a 20 wt.% YSZ suspension with time

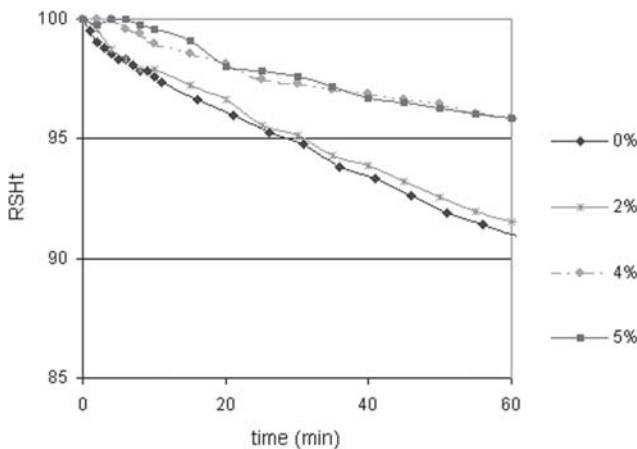


Fig. 3 Evolution of the sediment heights for various dispersant weight percentages in a suspension at 60 wt.% of YSZ

When the RSG is doubled, the distribution size remains bimodal, but the main peak is now centered at 30 μm and the peak shoulder is shifted toward around 150 μm . Finally, the droplet size distribution is a Gaussian-like curve centered around 25 μm that is obtained at RSG of 400.

Actually, during the atomization of a liquid by a gas, the gas creates disturbances in the liquid flow from outside to inside. At

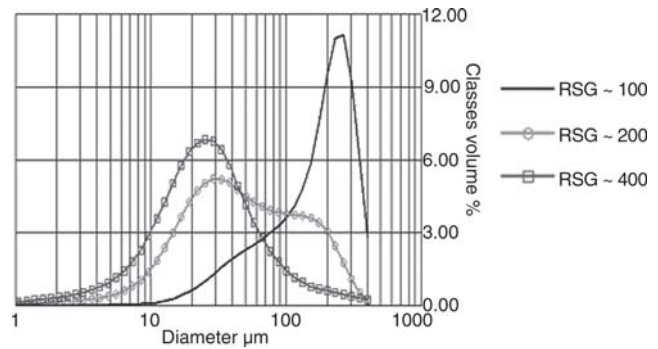


Fig. 4 Droplets size evolution as a function of RSG for a 20 wt.% YSZ suspension in methanol

the same time, the liquid is dragged along and thus drops are created (Ref 19). So, the increase of the argon flow rate or the decrease of the suspension feed rate has two consequences: to increase the liquid fragmentation speed that leads to smaller droplets and to allow the disturbances to be equal in all parts of the jet, so that the distribution is tightened. In this way, to quadruple the RSG value leads to a decrease in the drop size by a factor of ten and to a narrow drop size distribution.

The density of the suspension, related to the amount of solid particles, also influences the droplet size distribution as shown in Fig. 5. The size distribution for the 20 wt.% suspension is the monomodal curve centered at 25 μm . It seems that increasing the suspension solid content leads to a broadening of the distribution. The width of the distribution at half-height of the major peak is around 50 μm for the 20 wt.% YSZ suspension, 185 μm for the 40 wt.%, and 195 μm for the 60 wt.%. In addition, the distribution is also more chaotic when the load increases until a trimodal curve is observed for the distribution recorded for the 60 wt.% suspension.

This phenomenon can probably be explained because an increase of the suspension viscosity (associated with the increase of the solid content) prevents the disturbances caused by the argon flow from homogeneously affecting the liquid flow. The jet center is less disturbed, and bigger drops are produced. So the droplet sizes are more irregular, and consequently the distribution is larger.

This trend can be countered by the addition of a dispersant that improves the flow of the suspension and thus has the opposite effect (Fig. 6). The dispersant has indeed decreased the suspension viscosity as shown in the previous paragraph, thus allowing the atomization to be more homogeneous.

3.3 Influence of the Spraying Distance

The spraying distance was varied from 40 to 60 mm using standard spraying conditions with a suspension containing 20 wt.% YSZ particles and an atomizing parameter RSG of 100. SEM images of both coatings presented in Fig. 7 show that the thickness increases slightly as the spraying distance decreases. Furthermore, the microstructures of these coatings are different. With a 60 mm spraying distance, the layer is composed of an alternation of dense and porous features leading to a total volume porosity of 36%, while at 40 mm the coating is still porous

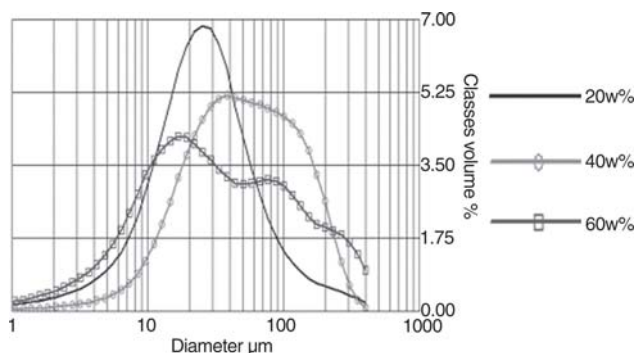


Fig. 5 Droplet size distribution for various suspension loading at RSG 400

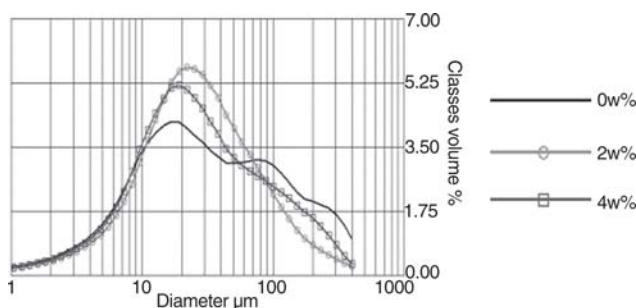


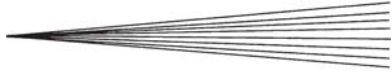
Fig. 6 Droplet size distribution for 60 wt.% suspensions with various amounts of Solsperce 20000 at RSG 400

but the dense features are more important, leading to a lower porosity of 26%. The porous regions were investigated by SEM, as reported in Fig. 8. At 60 mm, they seem to be constituted of nonmelted particles with sharp shapes and cooled round particles. The nonmelted particles are originated either from particles that were not heated enough or from overspraying during the injection. The spherical particles that are embedded in the coating correspond to particles that were melted and cooled down before impacting on the substrate. In contrast, the porous regions of the coating made at 40 mm do not show cooled particles.

3.4 Effects of the Droplets Size on the Coating Microstructure

Layers have been manufactured using different injection characteristics. First, a low RSG (100 achieved with a 40 mL/min suspension feed rate and a 4 L/min argon flow rate) has been chosen to produce large droplets (250 μm). A cross section of the coating produced using these atomizing conditions is shown in Fig. 7(a).

This layer thickness is around 50 μm (measured by image analysis). It also presents regions that are fully dense mixed with two types of porosity: large pores as can be seen on the top of the SEM view and regions containing particles and pores of relatively smaller dimensions. The total volume porosity was evaluated to be about 26%. The large pores are probably originated from the wrenching of cooled-down particles off the coating



during metallographic preparation. As they were not flattened, they created large cavities once the particles are pulled out. Figure 8(a) shows that the coating also presents smaller particles with sizes around 0.5 μm , which correspond to the starting particles. This means that the thermal transfer from the plasma to the drop and particles is not complete because the drop size is large, and depending on their trajectories inside the plasma plume they undergo more or less disintegration and melting. These particles can also come from overspraying of the suspension during the injection: droplets could have been ejected toward the substrate, dried, and then trapped in the coating.

A coating had also been manufactured with a RSG of 400 at a constant atomizing gas flow rate constant (with a 10 mL/min suspension feed rate and 4 L/min argon flow rate), leading to a narrow drop size distribution centered at 25 μm . The cross section presented in Fig. 9 shows that the coating is really thinner (around 15 μm), which almost corresponds to the decrease of the suspension feed rate (10 mL/min against 40 mL/min for RSG 100). Although the microstructure of the coating seems to be similar, the total volume porosity is slightly lower, around 23 vol.%. So it seems that the droplets have a slight influence on the microstructure: a narrower distribution of smaller droplets seems to allow a better penetration of the droplets in the plasma and results in a denser coating.

3.5 Effects of Atomizing Gas Flow Rate at RSG Constant on the Microstructure

Another coating was produced in the same conditions of RSG 400, but this time both the suspension feed rate and carrier gas flow rate were doubled (respectively, equal to 20 and 8 L/min). With the RSG remaining constant, the droplets are assumed to follow the same size distribution.

On the cross section view shown in Fig. 10, the layer appears to be four times thicker (around 60 μm) than the previous one. This increase is two times higher than what was expected due to the two-time increase of the suspension feed rate. This result is most probably due to the higher argon flow rate: with the quantity of movement of the droplets in this case being increased, they may have entered the plasma more easily. Thus the spraying efficiency was increased and a thicker coating was produced.

However its microstructure seems quite similar to that of the previous coating: dense parts are separated by large porosities while some smaller porous region coexisted. Also, the total volume porosity is increased up to 35%.

So it seems that the increase of the carrier gas flow rate is a good way to improve the spraying efficiency. However, this is most likely associated with the increase of the volume porosity.

3.6 Effects of the Solid Content on the Coating Microstructure

A coating sprayed from a suspension containing 60 wt.% powder and 4 wt.% Solsperce 20000 (viscosity around 9 cP) has been realized with a RSG of 400. In these conditions, the droplet size distribution is centered at 20 μm . The SEM cross section view of the coating shown in Fig. 11 shows that the layer thus obtained is thicker (145 μm) than the others. This value corresponds to three times the thickness obtained with a 20 wt.% sus-

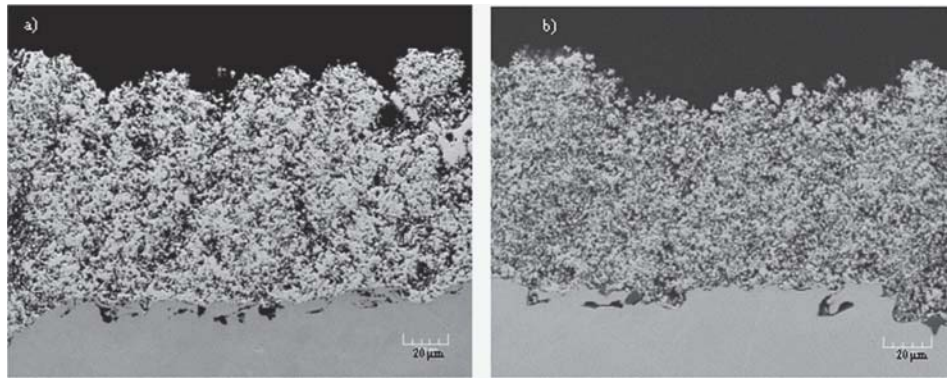


Fig. 7 SEM pictures of coatings produced with a RSG 100 at a spraying distance of (a) 40 mm and (b) 60 mm

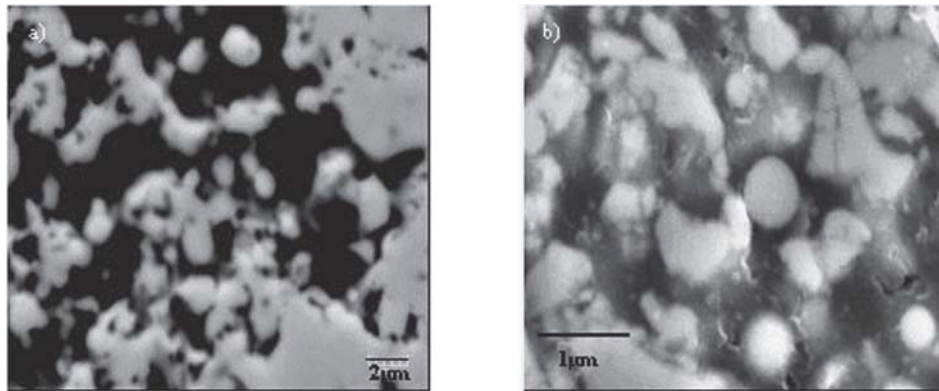


Fig. 8 SEM picture of the porous region for the coating sprayed at (a) 40mm and (b) 60 mm

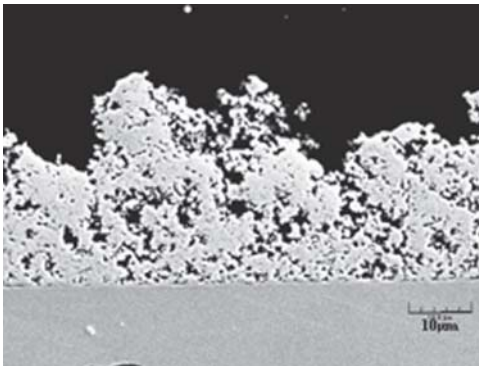


Fig. 9 SEM picture of the coating made with a RSG 400 (10 mL/min suspension, 4 L/min argon) with a 20 wt.% loaded suspension, injection characterized by small droplets

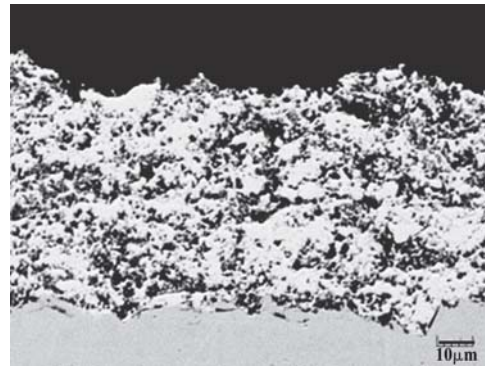


Fig. 10 SEM picture of the coating made with a RSG 400 (20 mL/min suspension, 8 L/min argon) with a 20 wt.% loaded suspension

pension, that is, to the increase of the solid content in the suspension. It also shows a fully composite microstructure with smaller dense parts, which explains the huge volume porosity measurement of 44%.

The porosity type has been also investigated by SEM, as shown in Fig. 12.

Here, the porous regions only contain small hard-shaped particles. So the porosity is only originated from nonmelted mate-

rials. Increasing the solid content of the suspensions gives drops that are much more difficult to melt. Indeed, considering the drops have the same size when they are in the plasma, those for which the solid content is higher will need more energy to melt as it is related with this quantity.

This means that a suspension with 60 wt.% particles would give a higher output. However, this suspension should be sprayed with a more energized plasma to be able to melt the particles and obtain fully dense coatings.

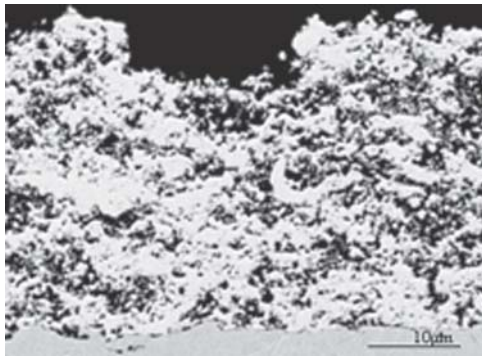


Fig. 11 SEM picture of the coating obtained with a 60 wt.% suspension at RSG 400

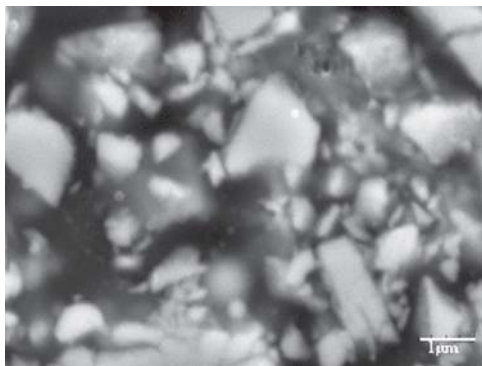


Fig. 12 SEM picture of porosity from coating with 60 wt.% suspension

3.7 Effects of the Particles Size in the Suspension

Another yttria-stabilized zirconia powder made of very fine particles (d_{50} 0.5 μm), from Umicore company (Asnières, France), has been used to produce suspension. The coating was realized with the same spraying standard conditions and a RSG of 100. The cross section view shown in Fig. 13 reveals that the thickness is similar to the one obtained with a powder with d_{50} around 0.6 μm . It also shows that the coating made with these fine particles seems to be less porous and more homogeneous. This observation is objected by the total volume porosities, which were evaluated to be around 26% in both cases. In fact, the difference in microstructure might come from a better melting of the droplets during the spraying due to the lower size of the particles in suspension.

4. Conclusions

An attempt was made in the current study to correlate the suspension characteristics, the suspension atomization and injection into the plasma, and the coating microstructural features.

Stability of the suspension seems to be enhanced by increasing the solid content. After 20 min of sedimentation, only 10 vol.% of a 60 wt.% YSZ suspension has settled, whereas 85 vol.% of a 20 wt.% YSZ suspension has settled. Besides it was noticed that the distribution size of the particles in these suspen-

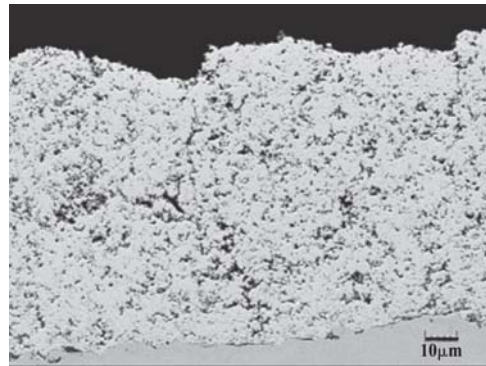


Fig. 13 SEM picture of the coating obtained with a 20 wt.% suspension containing particles with d_{50} 0.47 μm , at RSG 100

sions are bimodal with an increase of the large particles with time. Adding a dispersant, Solsperce 20000 for instance, seems to promote the dispersion of the particles inside the suspension.

Plasma sprayed coatings were realized by injecting these suspensions after atomization in a two-fluid nozzle specially designed for the suspension plasma spraying process. The influence of the spraying distance and the suspension, associated with the drop size distribution on the coating microstructure, were evaluated. The spraying distance is a key parameter to achieve dense and cohesive coatings. Furthermore, the atomization gas flow seems to have a great influence on the penetration of the drops inside the plasma jet and thus on the coating microstructure and the spraying efficiency, while the lower and narrower droplet size distributions improve the coating total volume porosity only slightly. Finally, using finer particles in suspension is supposed to be an interesting track to obtain denser coatings.

Acknowledgments

Technical assistance by M. Diraison from Malvern France, Solsperce 20000 provided by M. Richet from Noveon Company, France, and zirconia powder provided by M. Lerenard from Umicore Company, France, are gratefully acknowledged.

References

1. S.P.S. Badwal and K. Foger, Solid Oxide Electrolyte Fuel Cell Review, *Ceram. Int.*, 1996, **22**, p 257-265
2. P. Fauchais, V. Rat, C. Delbos, J.-F. Coudert, T. Chartier, and L. Bianchi, Understanding of Suspension DC Plasma Spraying Coatings for SOFC, *IEEE Trans. Plasma Sci.*, 2005, April 33(2)
3. C. Delbos, J. Fazilleau, V. Rat, J.-F. Coudert, P. Fauchais, and L. Bianchi, Influence of Powder Size Distribution and Heat Flux on Yttria Stabilised Coatings Elaborated by Liquid Suspension Injection in a DC Plasma Jet, *Thermal Spray 2005: Thermal Spray Connects: Explore Its Surfacing Potential!*, May 2-4, 2005 (Basel, Switzerland), E. Lugscheider, Ed., DVS, 2005
4. M. Bonneau, F. Gitzhofer, and M. Boulos, SOFC/CeO₂ Doped Electrolyte Deposition, Using Suspension Plasma Spraying, *Thermal Spray: Surface Engineering via Applied Research*, C.C. Berndt, Ed., ASM International, 2000
5. F. Gitzhofer, M. Bonneau, and M. Boulos, Doubled Doped Ceria Electrolyte Synthesized by Solution Plasma Spraying with Induction Plasma Technology, *Thermal Spray 2001: New Surfaces for a New Millennium*,

- C.C. Berndt, K.A. Khor, and E.F. Lugscheider, Ed., ASM International, 2001
6. J. Oberste Berghaus, S. Bouaricha, J.G. Legoux, and C. Moreau, Injection Conditions and In-Flight Particle States in Suspension Plasma Spraying of Alumina and Zirconia Nano-Ceramics, *Thermal Spray 2005: Thermal Spray Connects: Explore Its Surfacing Potential!*, May 2-4, 2005 (Basel, Switzerland), E. Lugscheider, Ed., DVS, 2005
 7. J. Oberste Berghaus, S. Bouaricha, J.G. Legoux, C. Moreau, and T. Chraska, Suspension Plasma Spraying of Nano-Ceramics Using an Axial Injection Torch, *Thermal Spray 2005: Thermal Spray Connects: Explore Its Surfacing Potential!*, May 2-4, 2005 (Basel, Switzerland), E. Lugscheider, Ed., DVS, 2005
 8. R. Siegert, J.-E. Döring, J.-L. Marqués, R. Vaßen, D. Sebold, and D. Stöver, Denser Ceramic Coatings Obtained by the Optimization of the Suspension Plasma Spraying Technique, *Thermal Spray 2004: Thermal Spray Solutions Advances in Technology and Applications*, (Osaka, Japan), May 10-12, 2004
 9. D. Stöver, D. Hathiramani, R. Vaßen, and R.J. Damani, Plasma Sprayed Components for SOFC application, 2005, *Proc. 2 Rencontres Internationales sur la Projection Thermique* (Lille, France), December 1-2, 2005
 10. M. Lang, R. Henne, S.E. Pohl, G. Schiller, and E. Hubig, Vacuum Plasma Spraying of Thin Film Planar Solid Oxide Fuel Cells (SOFC) Development and Investigation of the YSZ Electrolyte Layer, *International Thermal Spray Conference*, (Essen, Germany), March 4-6, 2002, E. Lugscheider, Ed., 2002
 11. G. Schiller, R.H. Henne, M. Lang, R. Ruckdschel, and S. Schaper, Development of Vacuum Plasma Sprayed Thin Film SOFC for Reduced Operating Temperature, *Fuel Cell Bull.*, 2000, 21
 12. X.Q. Ma, J. Roth, T.D. Xiao, and M. Gell, Study of Unique Microstructure in SPS Ceramic NanoCoating, *Thermal Spray 2003: Advancing the Science and Applying the Technology* (Orlando, FL), May 5-8, 2003, C. Moreau and B. Marple, Ed., ASM International, 2003
 13. X.Q. Ma, S. Hui, and H. Zhang, J. Dai, J. Roth, T.D. Xiao, and D.E. Reisner, Intermediate Temperature SOFC Based on Fully Integrated Plasma Sprayed Components, *Thermal Spray 2003: Advancing the Science and Applying the Technology*, May 5-8, 2003 (Orlando, FL), C. Moreau and B. Marple, Ed., ASM International, 2003
 14. C. Delbos, J. Fazilleau, J.F. Coudert, P. Fauchais, L. Bianchi, and K. Wittman-Teneze, Plasma Spray Elaboration of Finely Structured YSZ Thin coating by Liquid Suspension Injection, 2003, *Thermal Spray 2003: Advancing the Science & Applying the Technology*, May 5-8, 2003 (Orlando, FL), C. Moreau, and B. Marple, Ed., ASM International, 2003, p 661-669
 15. J. Fazilleau, "Contribution à la Compréhension des Phénomènes Impliqués dans la Réalisation de Dépôts Finement Structurés d'oxydes par Projection de Suspension Plasma," Ph.D. thesis, Limoges, France, 2003, in French
 16. E. Bouyer, F. Gitzhofer, and M.I. Boulos, Powder Processing by Suspension Plasma Spraying, *Thermal Spray: A United Forum for Scientific and Technological Advances*, C.C. Berndt, ASM International, 1997, p 353-359
 17. K. Wittman-Teneze, "Etude de l'élaboration de Couches Minces par Projection Plasma," Ph.D. thesis, Limoges, France, 2001, in French
 18. F.-L. Toma, "Elaboration et mise en forme de matériaux à base de TiO₂ pour le développement de traitements passifs de l'environnement (Application aux oxydes d'azote)," Ph.D. thesis, 2004, in French
 19. I. Filkkova and P. Cedik, Nozzle Atomization in Spray Drying, *Advances in Drying*, A.S. Mujumdar, Ed., Hemisphere Publishing Corp., Vol 3, 1984